W/Z production and properties

P. Pétroff

W and Z Production and Properties

Pierre Pétroff

Laboratoire de l'Accélérateur Linéaire B.P. 34 Orsay 91898 France

Abstract

Electroweak precision measurements performed by CDF and DØ are reported, corresponding to data collected at the center-of-mass energy of 1.96 TeV with the integrated luminosity ranging from 0.75 fb^{-1} to 4.9 fb^{-1}. These include the measurement of the W boson charge asymmetry, the measurement of the Z boson rapidity distribution, the measurement of the Z boson p_T distribution, and direct measurement of the W boson mass and width.

1. Introduction

The study of the electroweak gauge bosons W and Z is an important part of the physics programs at the Tevatron. Their large production rates and clean experimental signatures in leptonic decay modes facilitate several important measurements, such as the determination of the electroweak parameters M_W and Γ_W and the extraction of the parton distribution functions of the proton.

These decay modes are characterized by a high transverse energy lepton p_T^l and large transverse missing energy $\not\!\!E_T$ for W, or by two high transverse energy leptons for Z.

Electrons are identified as an electromagnetic (EM) cluster using a simple cone algorithm. To reduce the background of jets faking electrons, electron candidates are required to have a large fraction of their energy deposited in the EM section of the calorimeter and pass energy isolation and shower shape requirements. Electron candidates are classified as *tight* if a track is matched spatially to EM cluster and if the track transverse momentum is close to the transverse energy of the EM cluster. In CDF [1], electrons are reconstructed both in the central calorimeter and plug calorimeter ($|\eta| < 2.8$) while electrons in DØ [2] are reconstructed in the central and endcaps calorimeters ($|\eta| < 1.05$ and $1.5 < |\eta| < 3.2$). Here $\eta = -\ln\tan(\theta/2)$, and θ is the polar angle with respect to the proton direction. Both CDF and DØ require *tight* electrons in the central calorimeter ($|\eta| < 1.05$) for $Z \to e^+e^-$ candidates.

Muons are identified by a track in the muon system matched to a track in the central tracking system. For CDF the measurement in the muon channel includes the muons reconstructed in the central muon extension subdetector which extends the coverage from $|\eta| < 0.6$ to $|\eta| < 1$. For DØ the muon reconstruction is extended to the forward muon detector with a coverage up to $|\eta| = 2.0$. Muons from the decay of heavy-flavor hadrons are significant background to vector bosons production. It can be reduced by requiring that the muon is isolated. Cosmic ray muons contaminate the muon sample. Timing capabilities and distance of the muon track to the vertex are used to reduce the cosmic-ray muons background to low level.

We describe recent results from CDF and DØ collaborations. Two that constrain the parton distribution function (PDF) of the proton, the W boson charge asymmetry and the Z boson rapidity measurements, one that contrains the prediction of quantum chromodynamics (QCD), the Z boson p_T distribution measurement and two precision measurements of the W boson mass and width.

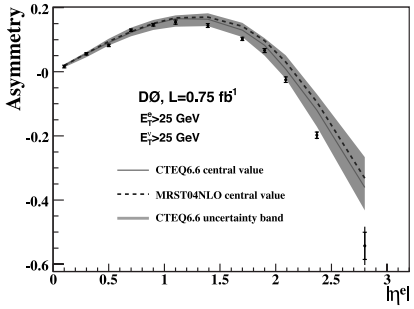

Fig. 1 DØ folded electron charge asymmetry distribution. the horizontal bars show the statistical uncertainty and the full vertical lines show the total uncertainty on each point. The solid line is the theoretical prediction for the asymmetry using CTEQ6.6 NLO central PDF set. The dashed line shows the same prediction using the MRST04 NLO PDFs. The shaded band is the uncertainty band using CTEQ6.6 PDF uncertainty sets.

2. W Boson Charge Asymmetry

Direct Measurement of W boson charge asymmetry provides new input on the momentum fraction dependence of the u and d quark parton distribution function within the proton.

As the u quark tends to carry a higher fraction of the proton's momentum than the d quark, the $W^+(W^-)$ is boosted, on average, in the proton(anti-proton) direction.

The $W^\pm$ charge asymmetry is defined as

$$A(y_W) = \frac{d\sigma(W^+)/dy_W - d\sigma(W^-)/dy_W}{d\sigma(W^+/dy_W) + d\sigma(W^-)/dy_W}$$

Measurements are typically performed using the charged leptons (e or μ) for the W boson decays. Since the longitudinal momentum of the neutrino is unmeasured, the asymmetry has been measured traditionally as

$$A(\eta_l) = \frac{d\sigma(l^+)/d\sigma\eta_l - d\sigma(l^-)/d\sigma\eta_l}{d\sigma(l^+)/d\sigma\eta_l + d\sigma(l^-)/d\sigma\eta_l}$$

where η_l is the lepton pseudorapidity. The lepton asymmetry, $A(\eta_l)$ is the convolution of $W^\pm$ production and V-A (vector-axial vector) decay asymmetries.

The DØ collaboration has recently published [5] results obtained from more than twice the integrated luminosity of previous measurements by the CDF [3] and DØ [4] collaborations and extend the measurement for electrons with $|\eta|^e < 3.2$. By extending the higher rapidity electrons, more information is provided about PDFs for a broader x range ($0.002 < x < 1.0$ for $|y_W| < 3.2$) at high $Q^2 \sim M_W^2$, where Q^2 is the momentum transfer squared, x is the fraction of momentum of the proton carried by the parton and M_W is the W boson mass. The integrated luminosity is 0.75 fb^{-1}.

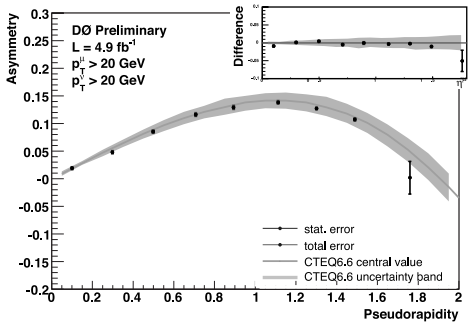

Fig. 2 DØ folded muon charge asymmetry distribution. The shaded band is the envelope determined using forty CTEQ6.1M PDF uncertainty sets, the solid (red) line is the CTEQ6.1M central value, and the dotted (blue) line is the charge asymmetry determined using MRST04 NLO PDFs.

The asymmetry measurement is sensitive to misidentification of the electron charge. The charge misidentification rate is measured with $Z \to ee$ events. The rate ranges from 0.2% at $|\eta| \sim 0$ to 9% at $|\eta| \sim 3$. The absolute uncertainty in the charge misidentification ranges from 0.1% to 2.6% depending on the electron rapidity and is dominated by the statistics of the Z boson sample. Assuming A(-η^e) = -A(η^e) due to CP invariance, data are folded to increase the available statistics. Fig. 1 shows the folded electron charge assymetry with theoretical predictions. These predictions are obtained using RESBOS event generator [6] (with gluon resummation at low boson p_T and NLO perturbative QCD calculations at high boson p_T) with PHOTOS [7] (for QED final state radiation). The PDFs used to generate these predictions are the CTEQ6.6 NLO PDFs [8] and MRST04 NLO PDFs [9]. The asymmetric PDF uncertainty band is calculated using the formula described in Ref. [10].

The experimental uncertainties are smaller than the theoretical predictions across almost all electron pseudorapidities and these results can be used to improve the precision and accuracy of next generation PDF sets. Fig. 2 shows a new preliminary DØ measurement of the lepton charge asymmetry using $W \to \mu\nu$ from 4.9 fb^{-1} data sample. The measured asymmetry is compared to a theoretical prediction based on CTEQ6.6 PDF model [8]. The results can already improve constraints on PDFs, especially for $0.7 < |\eta^\mu| < 1.6$. The charge asymmetry results presented above are made as a function of pseudorapidity of the leptons from W decay and the lepton charge asymmetry is a convolution of the W production charge asymmetry and the V-A asymmetry from W decays. These two asymmetries tend to cancel at large pseudorapidities ($|\eta| > 2.0$), and the convolution complicates the constraint on the proton PDFs. CDF has used a new analysis technics [11] to publish [12] the first direct measurement of the W production charge asymmetry in the $W \to e\nu$ decay channel with an integrated luminosity of 1.0 fb^{-1}. This method fully exploits the kinematic information in W events to directly reconstruct the underlying W boson production asymmetry. The W boson rapidity is ambiguous since the longitudinal momentum of the neutrino from its decay cannot be measured. However the neutrino momentum can be determined to a two-fold ambiguity by constraining the W boson mass.This ambiguity can be partly solved on a statistical basis from the known V-A decay distribution and the $W^\pm$ production cross section as a function of y_W and $d\sigma/dy$.

Fig. 3 shows the measured asymmetry A($|y_W|$, which combines the positive and negative y_W bins. The theroretical predictions at NNLO QCD calculation using the MRST2006 NNLO PDF sets [13] and a NLO QCD calculation using the CTEQ6.1 NLO PDF sets [14] are also shown. The CDF direct asymmetry measurement

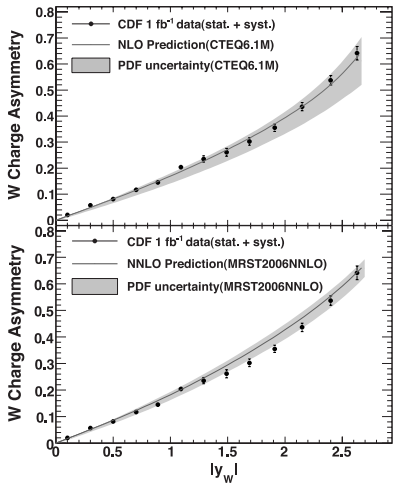

Fig. 3 CDF direct measured asymmetry, A$|y_W|$ with prediction from NLO CTEQ6.1 (top) and NNLO MRST2006 (bottom) with their associated PDF uncertainties

method indicates the possibility of a significant increase in sensitivity. In conclusion the charge asymmetry measurements from CDF and DØ collaborations will help to reduce the PDF uncertainty for high precision M_W measurements and also improve the predictions for the Higgs boson production at the hadron colliders.

3. *Z* Boson Rapidity

Measurement of the differential boson production cross section over the full rapidity range provide stringent constraints on PDF parametrizations. The dilepton decay modes of the Z boson allow for precise measurements, since backgrounds in these final states are small, and the full event kinematics can be precisely reconstructed.

At leading order Z/γ^* bosons are produced through the annihilation of a quark and an anti-quark, with the partons in the proton and anti-proton carrying momentum fractions x_1 and x_2, respectively. The rapidity of the boson, defined as $y = \frac{1}{2}\ln\frac{E+p_L}{E-p_L}$, where E is the energy of the boson and p_L is its longitudinal component, is directly related to the momentum fractions by $x_{1,2} = \frac{M_{Z/\gamma^*}}{\sqrt{s}}e^{\pm y}$. Here, M_{Z/γ^*} is the mass of the boson, and $\sqrt{s}$ is the center of mass energy. The forward rapidity region $|y| > 1.5$ probes quarks with low x and high 4-momentum transfer squared Q^2 ($Q^2 \approx M_Z^2$) as well as quarks with very large x.

CDF has made a measurement of the differential cross section $1/\sigma\frac{d\sigma}{dy}$, using 2.1 fb^{-1} of $Z \to ee$ data with $|\eta| < 2.8$. The total cross section, derived from integrating $d\sigma/dy$ up to $|y| < 2.8$, is $\sigma = 256.0 \pm 0.7(\text{stat}) \pm 2.0(\text{syst}) \pm 15.1(\text{lum})$ pb. The measured total cross section is consistent with both NLO and NNLO calculations. Fig. 4 shows the measured $d\sigma/dy$ values, which are symmetric about $y = 0$. The results are compared to QCD predictions at NLO with CTEQ6.1M [15], MRST2001E [16] PDFs and at NNLO with MRST2006 [13] PDFs. Fig. 5 shows the ratios of the measured $d\sigma/dy$ to theory calculated at NLO with CTEQ6.1M PDFs and at NNLO with MRST2006 PDFs. The experimental $d\sigma/dy$ is larger than the theoretical prediction at large

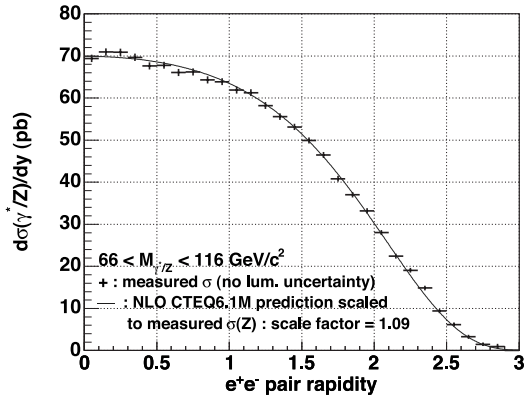

Fig. 4 The measured $d\sigma/dy$ over the entire rapidity range. The points are the measured cross sections versus dy and the solid line is the theory prediction (scaled to the measured total cross section) for CTEQ6.1M NLO PDFs.The 6% uncertainty in the integrated luminosity is not included in the error bars.

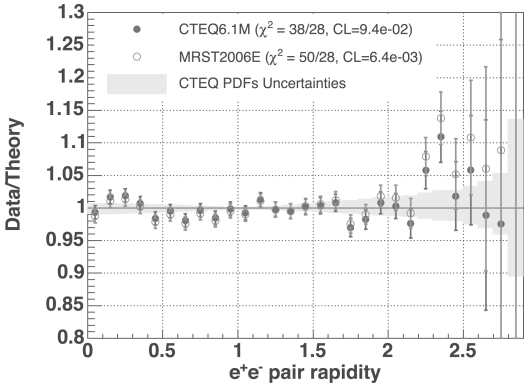

Fig. 5 The ratio of experimental distribution of $d\sigma/dy$ to the theoretical predictions for CTEQ6.1M(NLO), and MRST2006(NNLO) PDF models. The shaded band corresponds to the PDF's uncertainty obtained from CTEQ6.1M PDFs.

rapidities. Additional tuning of both NLO and NNLO PDF models may be needed.

4. *Z* Boson Transverse Momentum Study

Z boson production serves as an ideal testing ground for predictions of QCD at higher order calculations. A good understanding of electroweak vector boson production is important in precision measurement of W mass. The boson's transverse momentum, p_T^Z, can be measured over a wide range of values and can be correlated with its rapidity. At low p_T^Z the emission of multiple soft gluons is important and calculations in fixed order perturbative QCD diverge. A soft gluon emission resummation technique has been developed by Collins, Soper and Sterman (CSS) [17]. The resummation includes the BLNY [18] non-perturbative form factor that needs to be determined from data. The p_T^Z distribution at the Tevatron is sensitive to g_2, one of the phenomenological parameters of the form factor and almost insensitive to g_1 and g_3, the two other free parameters.

DØ has recently measured the g_2 parameter using di-muon and di-electron channels with 2 fb^{-1}. A novel technique has been used which allows to built an observable that is less sensitive to the resolution and more sensitive to the angular resolution, considering that collider detector generally have far better angular resolution than calorimeter or track transverse momentum resolution.

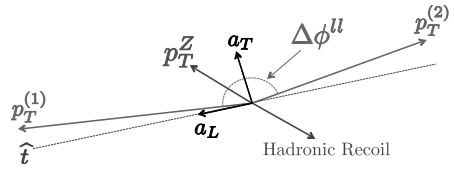

Fig. 6 A schematic representation in the transverse plane, of the constructionof a_T and a_L in a typical leptonic Z decay

The event axis (see Fig. 6) is defined as : $\hat{t} = \frac{\vec{p_T^1} - \vec{p_T^2}}{|\vec{p_T^1} - \vec{p_T^2}|}$ where $\vec{p_T^i}$ is the transverse momentum vector of lepton i. The transverse momentum of the di-lepton system, $\vec{p_T^Z}$ is decomposed into component transverse to the axis $\hat{t}$, $a_T = |\vec{p_T^Z} \times \hat{t}|$, and aligned with the axis, $a_L = \vec{p_T^Z} \cdot \hat{t}$. The a_T observable which has previously been used at LEP by the OPAL collaboration [19] is almost insensitive to the transverse momentum resolution of the individual leptons [20]

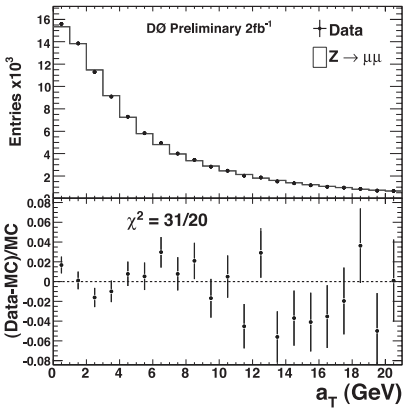

Fig. 7 Comparison of the di-muon data with MC simulation for a_T

Fig. 7 shows the a_T distributions for di-muons events. Data are fitted to PYTHIA [21] Monte Carlo templates weighted with RESBOS [6] using CTEQ6.6 [8] PDFs and PHOTOS [7] (for QED radiative corrections). Finally the combined measurement is: $g_2 = 0.63 \pm 0.02 \pm 0.04$ GeV^2. The first uncertainty is experimental and the second uncertainty is due to PDF dependence of the theroretical prediction. This measurement is compatible with the world average: $g_2 = 0.68^{+0.02}_{-0.01}\ GeV^2$ which does not include the PDFs uncertainty.

5. *W* Mass Measurement

A precision measurement of the W boson mass (M_W) is of the highest priority for the Tevatron experiments.

The W boson mass, combined with precise measurement of the top quark mass (M_{top}), constrains the mass of the Higgs boson. Self-energy corrections to the W boson depend on the masses of the top quark ($\propto M_{top}^2$) and the Higgs boson ($\propto \ln M_H$), as well as potential contributions from non-SM physics [22, 23].

The combined CDF and DØ result [24] on the top quark mass is 173.1 ± 1.3 GeV. The uncertainty corresponds to roughly a 0.75% measurement of M_{top}. For equal contribution to the Higgs boson mass uncertainty, The W boson mass would need to be measured to about 0.01% corresponding to a total uncertainty of 8 MeV.

The current world-average measured value is $M_W = 80.399 \pm 0.025$ GeV from a combination of measurements

from ALEPH [25], DELPHI [26], L3 [27], OPAL [28], CDF [29, 30] and DØ [31] collaborations.

We will report here a more recent measurement of M_W by the DØ collaboration [32] in the $W \to e\nu$ decay mode with an integrated luminosity of 1 fb^{-1}. This W mass is measured using three kinematic variables measured in the plane perpendicular to the beam direction: the transverse mass $m_T = \sqrt{2p_T^e p_T^\nu (1-\cos\Delta\phi)}$, the lepton ($p_T^e$) and neutrino ($p_T^\nu$) transverse momentum distributions, where $\Delta\phi$ is the opening angle between the electron and neutrino momenta in the plane transverse to the beam. The magnitude and direction of p_T^ν is inferred from the missing transverse energy ($\vec{\not\!\!E}_T$).

In order to select W boson data with low background and well-understood charged electron and neutrino kinematics, p_T^e and $\not\!\!E_T$ are required to be greater than 25 GeV, and recoil energy in the calorimeter is required to be less than 15 GeV. Moreover the electron is required to be in the central calorimeter with $|\eta| < 1.05$.

A sophisticated parametrized Monte Carlo simulation is used to predict the shape of the transverse mass distribution as well as the lepton and neutrino p_T distributions as a function of M_W. The W boson mass is extracted by fitting the M_W prediction of the Monte Carlo simulation to the data with a binned maximum-likelihood fit.

The lineshape predictions depend on a number of physical and detector effects, which can be constrained either from control samples or calculation. Important physical effects include internal QED radiation, the intrinsic W boson transverse momentum, and the proton parton distribution functions (PDF). Electron efficiency, hadronic recoil modelling, calorimeter response both to electromagnetic shower and hadronic shower and calorimeter fiducial acceptance are among the most important detector effects.

The major steps of the W mass measurement will be explained by the following:

Kinematics are simulated using the RESBOS [6] next-to-leading order generator which includes non-perturbative effects at low boson p_T. These effects are parametrized by three constants (g_1, g_2 and g_3) (as explained in Sec: 4.). Their values are taken from global fits to data [33]. The radiation of one or two photons is calculated using the PHOTOS [7] program.

Detector efficiencies, energy response and resolution for the electron and hadronic energy are applied to the RESBOS+PHOTOS events using a fast parametric Monte Carlo simulation (FASTMC) developed for this analysis. The FASTMC parameters are determined using a combination of detailed simulation and control data samples. The primary control sample used for both the electromagnetic and hadronic response tuning is $Z \to ee$ events. Since the Z boson mass and width are known with high precision from measurements [34] at the CERN e^+e^- collider (LEP), these values are used to calibrate the electromagnetic calorimeter response assuming a form $E^{meas} = \alpha\, E^{true} + \beta$ with α and β constants determined by calibration. The M_W measurement presented here is effectively a measurement of the ratio of W and Z boson masses. Fig. 8 shows a comparison of the m_{ee} distributions for data and FASTMC, as well as the χ distribution defined as the difference between data and the FASTMC prediction divided by the statistical uncertainty on the difference. Transverse recoil $\vec{u}_T$ is defined as all particles recoiling against the W or Z bosons. A combination of events recorded in random beam crossings, with or without requiring hits in the luminosity counters and $Z \to ee$ data is performed to describe the behavior of the hadronic recoil. Then the hadronic response (resolution) is tuned using the mean (width) of the η_{imb} distribution

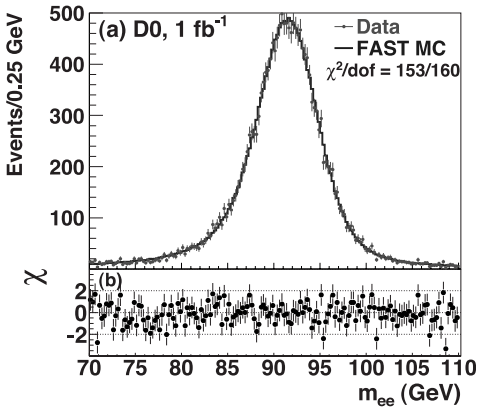

Fig. 8 (a) The dielectron invariant mass distribution in $Z \to ee$ data and from the fast simulation FASTMC and (b) the χ values where $\chi_i = [N_i - (\text{FASTMC}_i)]/\sigma_i$ for each point in the distribution, N_i is the data yield in bin i and σ_i is the statistical uncertainty in bin i.

in $Z \to ee$ events in bin of p_T^{ee}. Here η_{imb} is defined as the sum of the projections of the dielectrons momentum ($\vec{p}_T^{\,ee}$) and recoil momentum ($\vec{u}_T$) in the transverse plane on the axis ($\hat{\eta}$) bisecting the dielectron opening angle [35] (see Fig. 9). The backgrounds in the W boson sample are

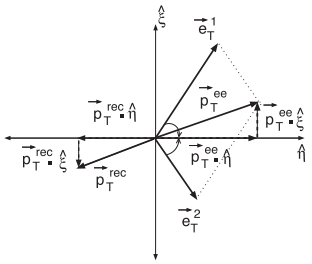

Fig. 9 Definition of η_{imb} for $Z \to ee$ events, as first defined by UA2 [35]. The $\hat{\eta}$ unit vector is coincident with the bisector of the two electron directions in the transverse plane.

$Z \to ee$ events in which one electron escapes detection, multijet events (MJ) in which a jet is misidentified as an electron with $\not\!\!E_T$ arising from misreconstruction, and $W \to \tau\nu \to e\nu\nu\nu$ events. The backgrounds expressed as a fraction of the final sample are $(0.90 \pm 0.01)\%$ from $Z \to ee$, $(1.49 \pm 0.03)\%$ from MJ, and $(1.60 \pm 0.02)\%$ from $W \to \tau\nu \to e\nu\nu\nu$.

The Z boson mass value from the final tuning fit is 91.185 ± 0.033 (stat) GeV, in agreement with the world average of 91.188 GeV used for the tuning. In Table 1 the results of the fit of the W mass are given together with the range of the fit and the χ^2 per degrees of freedom (dof). Fig. 10 shows the m_T distributions for the data and the FASTMC template with backgrounds and the bin-by-bin χ values defined as the difference between the data and the template divided by the data uncertainty. This FASTMC template corresponds to the best M_W fit.

Table 1 Results from the fits to data. The uncertainty is only the statistical component.

Variable	Fit Range (GeV)	M_W (GeV)	chi^2/dof
m_T	$65 < m_T < 90$	80.401 ± 0.023	48/49
p_T^e	$32 < p_T^e < 48$	80.400 ± 0.027	39/31
$\not\!\!E_T$	$32 < \not\!\!E_T < 48$	80.402 ± 0.023	32/31

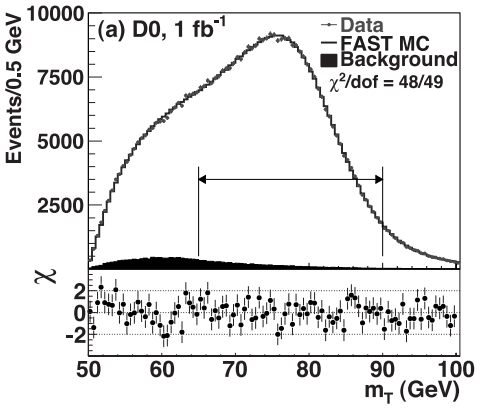

Fig. 10 The m_T distribution for DØ data and the fast simulation with backgrounds added (top), and χ value for each boin (bottom). The fit result is $m_W = 80.401 \pm 0.023$(stat) GeV.

The uncertainties on the electron energy calibration and the hadronic recoil model are determined by simultaneously varying the parameters determined in the tuning to $Z \to ee$ events by one statistical standard deviation including correlation coefficients. The electron energy resolution systematic uncertainty is determined by varying resolution parameters determined in the fit to the width of the observed $Z \to ee$ m_{ee} distribution. The shower modeling systematic uncertainties are determined by varying the amount of material representing the detector in the detailed simulation within the uncertainties found by comparing the electron showers in the simulation to those observed in data. The electron efficiency systematic is determined by varying the efficiency by one standard deviation. Table 2 also shows the M_W uncertainties arising from variation of the background uncertainties indicated above. Among the production uncertainties, the parton distribution function (PDF) uncertainty is determined by generating W boson events with the PYTHIA [21] program using the CTEQ6.1M [15] PDF set. The CTEQ prescription [36] is used to determine a one standard deviation uncertainty [12] on M_W. The QED uncertainty is determined using WGRAD [37] and ZGRAD [38], varying the photon-related parameters and assessing the variation in M_W and by comparisons between these and PHOTOS. The boson p_T uncertainty is determined by varying g_2 by its quoted uncertainty [33]. Variation of g_1 and g_3 has negligible impact. The quality

Table 2 Systematic uncertainties of the M_W measurement.

	ΔM_W (MeV)		
Source	m_T	p_T^e	$\not\!\!E_T$
Electron energy calibration	34	34	34
Electron resolution model	2	2	3
Electron shower modeling	4	6	7
Electron energy loss model	4	4	4
Hadronic recoil model	6	12	20
Electron efficiencies	5	6	5
Backgrounds	2	5	4
Experimental Subtotal	35	37	41
PDF	10	11	11
QED	7	7	9
Boson p_T	2	5	2
Production Subtotal	12	14	14
Total	37	40	43

of the simulation is indicated by the good χ^2 values computed for the difference between the data and FASTMC shown in the figures. The data are also subdivided into statistically independent categories based on instantaneous luminosity, time, the total hadronic transverse energy in the event, the vector sum of the hadronic energy, and electron pseudorapidity range. The fit ranges are also varied. The results are stable too within the measurement uncertainty for each of these tests. The results from the three methods have combined statistical and systematic correlation coefficients of 0.83, 0.82, and 0.68 for (m_T, p_T^e), (m_T, $\not\!\!E_T$), and (p_T^e, $\not\!\!E_T$) respectively. The correlation coefficients are determined using ensembles of simulated events. The results are combined [39] including these correlations to give the final result

$$\begin{aligned} M_W &= 80.401 \pm 0.021 \text{ (stat)} \pm 0.038 \text{ (syst) GeV} \\ &= 80.401 \pm 0.043 \text{ GeV}. \end{aligned}$$

The dominant uncertainties arise from the available statistics of the $W \to e\nu$ and $Z \to ee$ samples. Thus, this measurement can still be expected to improve as more data are analyzed.

The M_W measurement reported here agrees with the world average and the individual measurements and is more precise than any other single measurement. This new direct measurement has been combined with the previous CDF and DØ measurements. The new Tevatron result for the W boson mass is: $M_W = 80.420 \pm 0.031$ GeV. For the first time the total uncertainty from the Tevatron is smaller that of 0.033 GeV from LEP [40].

Fig. 11 shows the W boson mass measurement at LEP and Tevatron experiments as well as the world average: $M_W = (80.399 \pm 0.023)$ GeV. The result from the Tevatron corresponds to the value which includes corrections to the same W boson width and PDFs. The DØ value has been increased by one MeV to take into account these corrections. The updated world average impacts the global precision electroweak fits. By using this new world average only in the fit the Gfitter group [41] predicts that the Higgs mass is: $m_H = 42^{+295}_{-166}$ GeV. It predicts at 2 σ intervals that the Higs mass is included in the interval [114,153] GeV with a global precision electroweak fit including the LEP and Tevatron direct limits.

With more statistics, both experiments CDF and DØ are looking forward in the very near future, to measuring the W boson mass with a precision of the order of 25 MeV per experiment.

6. *W* Boson Width Measurement

A precise measurement of width (Γ_W) provides a stringent test of SM prediction which is accurate to 2 MeV [42]. The first Run II published result [43] on Γ_W has been presented by CDF with an integrated luminosity of .350 fb^{-1}. The W direct width measurement was determined to be $\Gamma_W = 2.032 \pm 0.071$ GeV by combining both the electron and muon decay channels. More recently DØ has performed a W direct width measurement with 1 fb^{-1} of data sample [44]. The measurement is performed in the $e\nu$ channel.

The analysis is very similar to the W mass analysis. A Monte Carlo simulation is used to predict the m_T distribution as a function of Γ_W. Then these predictions are fitted to the data with a binned maximum-likelihood fit to extract Γ_W. While the fit for M_W is performed in the region around the peak of the distribution (65-90 GeV), the fit for Γ_W is performed in the high m_T tail region (90-200 GeV). This region is sensitive to the Breit-Wigner line-shape and less sensitive to the detector resolution.

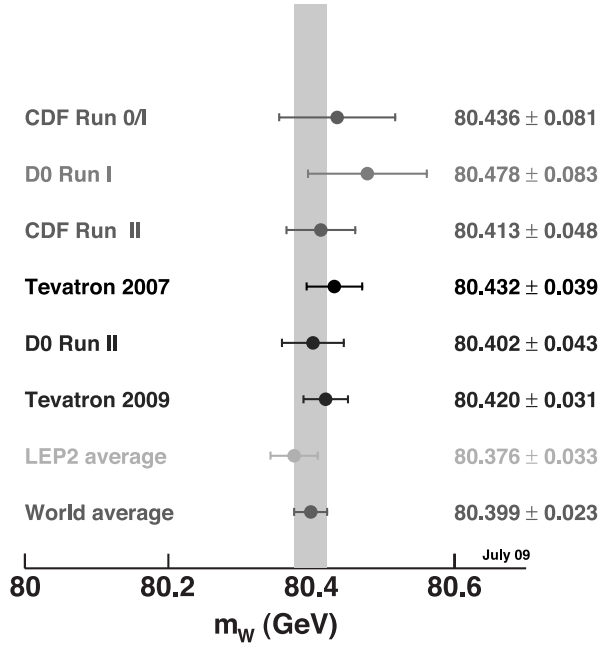

Fig. 11 Summary of the measurements of the W boson mass and their average. The result from the Tevatron corresponds to the values which includes corrections to the same W boson width and PDFs. The LEP II results is from [40]. An estimate of the world average of the Tevatron and LEPP results assuming no correlations between the tevatron and LEP is included.

The modeling of the recoil is based on the recoil library obtained from $Z \to ee$ events. A Bayesian unsmearing procedure [45] allows the transformation of the two-dimensional distribution of reconstructed Z boson p_T and the measured recoil momentum $\vec{u}_T$ to one between the true Z boson p_T and the measured recoil $\vec{u}_T$. For each simulated $W \to e\nu$ event with a generator-level transverse momentum value $\vec{p}_T$, we select $\vec{u}_T$ randomly from the Z boson recoil library with the same value of $\vec{p}_T$. Details can be found in [46]. The uncertainty on the recoil system simulation from this method is dominated by the limited statistics of the Z boson sample; other systematic uncertainties originate from the modelling of photon radiative corrections, acceptance differences between W and Z boson events, underlying energy corrections beneath the electron cluster, residual efficiency-related correlations between the electron and the recoil system, and the unfolding procedure.

Previous M_W and Γ_W measurements have relied upon parameterizations of the recoil kinematics based on phenomenological models of the recoil and detector response. The library method used here includes the actual detector response for the hadronic recoil and also the complex correlations between different components of the hadronic recoil. It requires no first-principles description of the recoil system and has no adjustable parameters. Table 3 gives the detailed breakdown of the systematic uncertainties. We fit the m_T data distribution to a set of templates at different assumed widths between a lower m_T value and $m_T = 200$ GeV. The lower m_T cut is varied from 90 to 110 GeV to test the stability of the fitted result. While the statistical uncertainty decreases as the lower m_T cut is reduced, the systematic uncertainty increases. The lowest overall uncertainty is obtained for a lower m_T cut of 100 GeV with $\Gamma_W = 2.028 \pm 0.039(\text{stat}) \pm 0.061(\text{syst})$ GeV. Fig. 12 shows the m_T distributions for the data and the FASTMC template with backgrounds and the bin-by-bin χ values defined as the difference between the data and the template divided by the data uncertainty. This FASTMC template corresponds to the best M_W fit.

Table 3 Systematic uncertainties on the measurement of Γ_W.

Source	$\Delta\Gamma_W$ (MeV)
Electron energy scale	33
Electron resolution model	10
Recoil model	41
Electron efficiencies	19
Backgrounds	6
PDF	20
Electroweak radiative corrections	7
Boson p_T	1
M_W	5
Total Systematic	61

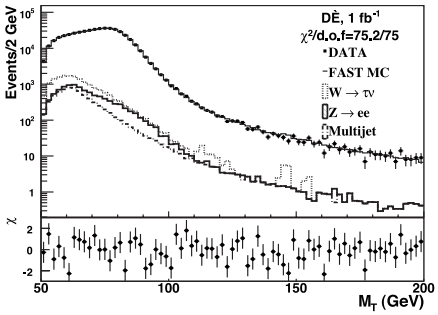

Fig. 12 The M_T distributions for data and fast MC simulation with background added (top) and the χ values for each bin (bottom). The fitted Γ_W value is used for the fast MC prediction. The distribution of the fast MC simulation with background added is normalized to the number of data events in the region $50 < M_T < 100$ GeV.

7. Conclusion

The analyses reported here are based on only a small fraction of the expected data. There is significant room for improving the precision of current measurement with around 10 fb^{-1} data sample expected at the completion of the Tevatron. Nevertheless, the large sample analysed up to now accommodate a wide variety of electroweak measurements. Future prospects in W mass measurement (≈ 25 MeV per experiment) will further constrain the Higgs mass.

8. Acknowledgments

It is a pleasure to thank my CDF and DØ colleagues for the exciting and fruitful collaboration, and our Tevatron colleagues for the excellent luminosity. I also thank very warmly the organisers for the very nice and interesting *XXIX PHYSICS IN COLLISION* conference.

References

[1] D. Acosta *et al.* (CDF Collaboration), Phys. Rev. D71 (2005) 032001.
[2] V. M. Abazov *et al.* (DØ Collaboration), Nucl. Instrum. Methods in Phys. Res. A565 (2006) 463.
[3] F. Abe *et al.* (CDF Collaboration), Phys. Rev. Lett. 74 (1995) 850; F. Abe *et al.* (CDF Collaboration), Phys. Rev. Lett. 81 (1998) 5754; D. Acosta *et al.* (CDF Collaboration), Phys. Rev. D74 (2005) 051104.

[4] V. M. Abazov *et al.* (DØ Collaboration), Phys. Rev. D77 (2008) 011106.
[5] V. M. Abazov *et al.* (DØ Collaboration), Phys. Rev. Lett. 101 (2008) 211801.
[6] C. Balazs, and C. P. Yuan, Phys. Rev. D56 (1997) 5558.
[7] E. Barberio, and Z. Was, Comput. Phys. Commun. 79 (1994) 291.
[8] P. M. Nadolsky *et al.*, Phys. Rev. D78 (2008) 013004.
[9] A. D. Martin, R. G. Roberts, W. J. Stirling, and R. S. Thorne, Phys. Lett. B 604 (2004) 61.
[10] D. Stump *et al.*, JHEP 0310 (2003) 046.
[11] A. Bodek, *etal.*, Phys. Rev. D77 (2008) 111301.
[12] T. Aaltonen *et al.* (CDF Collaboration), Phys. Rev. Lett. 102 (2009) 181801.
[13] A. Martin, J. Stirling, R. Thorne, and G. Watt, Phys. Lett. B 652 (2007) 292.
[14] J. Pumplin, D. R. Stump, J. Huston, H. L. Lai, S. Kuhlmann, J. F. Owens, and W. K. Tung, J. High Energy Phys. 0310 (2003) 046.
[15] J. Pumplin, D. R. Stump, J. Huston, H. L. Lai, P. Nadolsky, and W. K. Tung, JHEP (2002) 0207; J. Pumplin, D. R. Stump, J. Huston, H. L. Lai, W. K. Tung, S. Kuhlmann, and J. F. Owens, JHEP (2003) 0310:046.
[16] A. D. Martin, R. G. Roberts, W. J. Stirling, and R. S. Thorne, Eur. Phys. J. C 28 (2003) 455.
[17] J. Collins, D. Soper, and G. Sterman, Nucl. Phys. B259 (1985) 199.
[18] F. Landry, *et al.*, Phys. Rev. D67 (2003) 073016.
[19] K. Ackerstaff *et al.*, (OPAL Collaboration), Eur. Phys. JC4 (1998) 47.
[20] M. Vesterinen, and T. R. Wyatt, arXiv:0807.4956 [hep-ph] (2008).
[21] T. Sjöstrand *et al.*, Comput. Phys. Commun. 135 (2001) 238.
[22] W. J. Marciano, Phys. Rev. D20 (1979) 274; F. Antonelli, M. Consoli, and G. Corbo, Phys. Lett. B91 (1980) 90; M. Veltman, *ibid.*, (1980) 95.
[23] A. Stirlin, Phys. Rev. D22 (1980) 971.
[24] CDF and DØ Collaborations (combined top mass result), arXiv:0903.2503v1 [hep-ex] (2009).
[25] S. Schael *et al.* (ALEPH Collaboration), Eur. Phys. J. C 47 (2006) 309.
[26] J. Abdallah *et al.* (DELPHI Collaboration), Eur. Phys. J. C 55 (2008) 1.
[27] P. Achard *et al.* (L3 Collaboration), Eur. Phys. J. C 45 (2006) 569.
[28] G. Abbiendi *et al.* (OPAL Collaboration), Eur. Phys. J. C 45 (2006) 307.
[29] T. Affolder *et al.* (CDF Collaboration), Phys. Rev. D64 (2001) 052001.
[30] T. Aaltonen *et al.* (CDF Collaboration), Phys. Rev. Lett. 99 (2007) 151801; T. Aaltonen *et al.* (CDF Collaboration), Phys. Rev. D77 (2008) 112001.
[31] B. Abbott *et al.* (DØ Collaboration), Phys. Rev. D58 (1998) 092003; B. Abbott *et al.* (DØ Collaboration), Phys. Rev. D62 (2000) 092006; V. M. Abazov *et al.* (DØ Collaboration), Phys. Rev. D66 (2002) 012001.
[32] V. M. Abazov *et al.* (DØ Collaboration), Phys. Rev. Lett. 103 (2009) 141801.
[33] F. Landry, R. Brocks, P. Nadosky, and C. P. Yuan, Phys. Rev. D67 (2003) 073016.
[34] C. Amsler *et al.*, Phys. Lett. B 667 (2008) 1 and references therein.
[35] J. Alitti *et al.* (UA2 Collaboration), Phys. Lett. B 276 (1992) 354.
[36] H. L. Lai *et al.*, Phys. Rev. D55 (1997) 1280; D. Stump *et al.*, JHEP 0310 (2003) 046.
[37] U. Baur *et al.*, Phys. Rev. D59 013002 (1998) 013002.
[38] U. Baur *et al.*, Phys. Rev. D57 (1998) 199; U. Baur *et al.*, Phys. Rev. D65 (2002) 033007.
[39] L. Lyons, D. Gibout, and P. Clifford, Nucl. Instrum. Methods in Phys. Res. A270 (1988) 110; A. Valassi, Nucl. Instrumm. Methods in Phys. Res. A500 (2003) 391.
[40] The LEP Electroweak Working Group, CERN-PH-EP/2008-20, arXiv:0811.4682 [hep-ex].
[41] H. Flächer, M. Goebel, J. Haller, A. Hoecker, K. Mönig, and J. Stelzer, arXiv:0811.0009. More information is available at: http://cern.ch/gfitter.
[42] J. L. Rosner, M. P. Worah, and T. Takeuichi, Phys. Rev. D49 (1994) 1363.
[43] T. Aaltonen *et al.* (CDF Collaboration), Phys. Rev. Lett. 100 (2008) 071801.
[44] V. M. Abazov *et al.* (DØ Collaboration), arXiv.org:0909.4814 (2009) submitted to Phys. Rev. Lett.
[45] G. D'Agostini, Nucl. Instrum. Methods in Phys. Res. A362 (1995) 487.
[46] V. M. Abazov *et al.* (DØ Collaboration), Nucl. Instrum. Methods in Phys. Res. A609 (2009) 250.